Hydration Effects on the HET-s Prion and Amyloid-β Fibrillous Aggregates, Studied with Three-Dimensional Molecular Theory of Solvation

Takeshi Yamazaki,* Nikolay Blinov,*† David Wishart,*‡ and Andriy Kovalenko*†
*National Institute for Nanotechnology, Edmonton, Alberta, Canada; and †Department of Mechanical Engineering and ‡Departments of Computing Science and Biological Sciences, University of Alberta, Edmonton, Alberta, Canada

ABSTRACT We study the thermodynamic properties of the experimental fragments of the amyloid fibril made of the HET-s prion proteins (the infectious element of the filamentous fungus *Podospora anserina*) and of amyloid-β proteins (the major component of Alzheimer's disease-associated plaques) by using the three-dimensional molecular theory of solvation. The full quantitative picture of hydration effects, including the hydration thermodynamics and hydration structure around the fragments, is presented. For both the complexes, the hydration entropic effects dominate, which results in the entropic part offsetting the unfavorable energetic part of the free energy change upon the association. This is in accord with the fact that the hydrophobic cooperativity plays an essential role in the formation of amyloid fibrils. By calculating the partial molar volume of the proteins, we found that the volume change upon the association in both the systems is large and positive, with the implication that high pressure causes destabilization of the fibril. This observation is in good agreement with the recent experimental results. We also found that both the HET-s and amyloid-β pentamers have loose intermolecular packing with voids. The three-dimensional molecular theory of solvation predicts that water molecules can be locked in the interior cavities along the fibril axis for both the HET-s and amyloid-β proteins. We provide a detailed molecular picture of the structural water localized in the interior of the fibrils. Our results suggest that the interior hydration plays an important role in the structural stability of fibrils.

INTRODUCTION

The process of aggregation of fibrillous peptides and formation of amyloid fibrils have been intensively studied both experimentally and theoretically (1–8). The driving forces behind the oligomerization and stability of amyloid fibrils have been gradually uncovered. It is long believed that the hydrophobic cooperativity is one of the most important factors in the association of proteins along with formation of networks of hydrogen bonds, favorable dispersion interactions, and possibly, the aromatic interactions between peptides in the amyloid fibril. It has been recently proven in the numerical simulations (9) that accounting for the hydrophobic (including the solvent expulsion) effects and the hydrogen bonding can explain all the stages in the nucleation-condensation pathway (2,10,11) of the formation of the amyloid filament with its characteristic cross-β structural motif (12). The complexity of the problem, and the necessity to analyze aggregates of proteins composed of many peptides, make the study of the thermodynamics of the fibril formation and stability, based on the all-atom molecular dynamics approaches, a very challenging problem. Despite the fact that the results of many such studies have been reported recently (see, for example, (13–34)), most of them have dealt with the analysis of specific stages and pathways of the amyloidogenesis. Full quantitative description of the thermodynamics of oligomerization and formation of amyloid fibrils and their stability is still scarce.

To fill the gap, we propose to use the three-dimensional molecular theory of solvation, also known as the three-dimensional reference interaction site model (3D-RISM) (35–39), the statistical-mechanical approach proven to be successful in the description of the thermodynamics and solvation structural properties of, in particular, biological macromolecules under various solvent conditions (40–46). The method is a three-dimensional generalization of RISM theory pioneered by Chandler and Andersen (47) and Chandler (48) and employed by Yu et al. to develop full thermodynamic analysis and decomposition of solvation driving forces (49). The approach relies on the fact that the solvent degrees of freedom in the statistical-mechanical representation for the free energy can be partially integrated out and then can be treated in terms of the density-density distribution functions. The latter can be obtained, based on rigorous statistical-mechanical treatment using the integral equations formalism (Ornstein-Zernike theory (50)). An important component of the theory is a closure relation to the integral equation; we employ the Kovalenko-Hirata closure approximation (KH) which adequately reproduces both electrostatic and nonelectrostatic effects and features of solvation structure (35,38). The level of description inherent in 3D-RISM theory allows one to represent solvation in terms of the three-dimensional distribution functions of solvent molecules. The method accounts for solvation effects with the accuracy comparable to the explicit solvation molecular dynamics approaches, but with less computational efforts.

Submitted October 2, 2007, and accepted for publication July 22, 2008.

Address reprint requests to Andriy Kovalenko, Tel.: 780-641-1716; E-mail: andriy.kovalenko@nrc-cnrc.gc.ca.

Editor: Gregory A. Voth.

0006-3495/08/11/4540/09 $2.00

doi: 10.1529/biophysj.107.123000

Moreover, the solvation thermodynamics (the solvation free energy and its derivatives, including volumetric effects) can be obtained in analytical form, and thus they do not require any special treatment such as the perturbation and thermodynamic integration methods.

In this article, we analyze the solvation thermodynamics of the fragments of the amyloid fibrils made of the HET-s prion proteins and the amyloid-β (Aβ) peptides by using the 3D-RISM-KH theory. The HET-s prion protein is the infectious element of the filamentous fungus *Podospora anserina*. The high-resolution molecular structure of the rigid core of HET-s(218–289) prion fibrils has been recently determined in the solid-state nuclear magnetic resonance experiments (51). The fibril forms a left-handed β-solenoid with a triangular hydrophobic core (51). The Aβ peptides are the major component of the Alzheimer's disease-associated plaques. The three-dimensional molecular structure of the Aβ has been uncovered recently (52,53).

The article is organized as follows: In Methods, the 3D-RISM-KH theory and the experimental structures of the fragments of the fibrils made of the HET-s and Aβ proteins are briefly reviewed. In Results and Discussion, we provide the full quantitative description of the solvation effects on the stability of the both complexes. A special emphasis is given to the hydrophobic effects that are shown to provide a dominant contribution to the gain of the free energy upon the assembly of the fibril fragments. Then, we show that the volumetric effects are inherently linked to the pressure destabilization of the protein aggregates, which is in accord with the available experimental data. We also show that the fibril structures studied have loose intermolecular packing with voids. It is demonstrated that water molecules can penetrate into the interior cavities along the fibril axis, which is in agreement with the recent molecular dynamics study on the Aβ fibrils (14,15,19). To the best of our knowledge, the possibility of localization of water molecules inside the prion fibrils is identified here for the first time. We suggest that the interior hydration plays an important role in the structural stability of the fibrils. We make concluding remarks in the last section.

METHODS

Molecular models of amyloid fibrils

As an input to the thermodynamic calculations based on the three-dimensional molecular theory of solvation, molecular models of proteins are required. The experimental structure of the pentamer fragment of the filament made of the HET-s prion proteins (51) was provided by the authors. In this study, we used the lowest energy model from Fig. 2 *A* of the original article by Wasmer et al. (51). To model the fragment of the Aβ fibril, we started from the experimental structure (Protein Data Bank ID code 2BEG, model 1). The fragment consists of five Aβ(1-42) peptides (53). The coordinates of the residues from 17 to 40 for each monomer were taken from the Protein Data Bank file. The coordinates of missing atoms from the disordered regions were first built using the DiscoveryStudio 2.0/Biopolymer (Accelrys, San Diego, CA). Then, these regions (residues 1–16 and 41–42) were optimized with the program MODELLER (54,55). Before passing to MODELLER, the structure was energy-minimized with the AMBER 9 molecular dynamics package (56) and the ff03 protein force field (57,58) with the atoms from residues 17 through 40 restrained to the experimental coordinates. For the energy minimization, we used the all-atom model for the proteins and the generalized Born/surface area model for water (59,60). To reduce the effect of the noncompensated charge of the fragment (-3 for each Aβ(1-42) monomer), we set the salt concentration to 0.2 M. There was no cutoff for the nonbonded interactions. The other parameters were set to the default values. The minimization was repeated for the conformations with the optimized disordered regions (the output of the program MODELLER). It was found that up to four residues from these regions for each peptide form β-sheets that extend the original (experimental) β-sheet structure. This is in agreement with available nuclear magnetic resonance data (52). Before calculating the thermodynamic properties using the 3D-RISM approach, both the experimental structure of the HET-s fibril fragment and the Aβ pentamer were energy-minimized using the implicit solvation model (generalized Born/surface area at 0.2 M salt concentration) with all of the α-carbon atoms kept restrained. The convergence criterion for the energy gradient was set to 0.01 kcal/mol Å of the root mean-square of the Cartesian elements of the gradient.

Three-dimensional molecular theory of solvation: formalism and numerical details

The molecular theory of solvation in its three-dimensional version is a powerful tool to study solvation thermodynamics of macromolecules under different solvent conditions. In this section, we briefly review the key aspects of the theory that are relevant to the following discussion.

The 3D-RISM equation (35–39)

$$h_\gamma(\mathbf{r}) = \sum_{\gamma'} \int d\mathbf{r}' c_{\gamma'}(\mathbf{r}') \chi_{\gamma'\gamma}(|\mathbf{r} - \mathbf{r}'|) \tag{1}$$

is coupled with the three-dimensional version of the closure approximation proposed by Kovalenko and Hirata (3D-KH closure) (35,38,39):

$$g_\gamma(\mathbf{r}) = \begin{cases} \exp(d_\gamma(\mathbf{r})) & \text{for } d_\gamma(\mathbf{r}) \le 0 \\ 1 + d_\gamma(\mathbf{r}) & \text{for } d_\gamma(\mathbf{r}) > 0 \end{cases}, \tag{2a}$$

$$d_\gamma(\mathbf{r}) = -u_\gamma(\mathbf{r})/(k_B T) + h_\gamma(\mathbf{r}) - c_\gamma(\mathbf{r}). \tag{2b}$$

Here, $h_\gamma(\mathbf{r})$ is the three-dimensional total correlation function that is related to the three-dimensional distribution function $g_\gamma(\mathbf{r}) = h_\gamma(\mathbf{r}) + 1$. The latter gives the normalized excess/depletion of the solvent density of site γ (e.g., water oxygen or hydrogen) around the solute molecule with respect to the bulk-solvent density. The three-dimensional direct correlation function $c_\gamma(\mathbf{r})$ has the asymptotic of the solute-solvent site interaction potential: $c_\gamma(\mathbf{r}) \sim -u_\gamma(\mathbf{r})/k_B T$, where k_B is the Boltzmann constant and T is the temperature of the system. The solvent susceptibility $\chi_{\gamma'\gamma}(r) = \omega_{\gamma'\gamma}(r) + \rho_{\gamma'} h_{\gamma'\gamma}(r)$ splits up into the intramolecular distribution function $\omega_{\gamma'\gamma}(r)$, which specifies the geometry of the solvent molecules and the intermolecular part given by the site-site total correlation function $h_{\gamma'\gamma}(r)$ multiplied by the solvent site-number density $\rho_{\gamma'}$. The radial correlations $h_{\gamma'\gamma}(r)$ of pure solvent can be obtained in advance from the dielectrically consistent one-dimensional RISM integral equation theory (DRISM) (61) coupled with the KH closure (35,39). The convolution in Eq. 1 is calculated by using the three-dimensional fast Fourier transform technique, with the analytical treatment of the electrostatic asymptotics of all of the correlation functions (35,39).

Within the 3D-RISM-KH formalism, the integration over the coupling parameter in the thermodynamics integration representation for the excess chemical potential can be carried out in the explicit form. The hydration free energy of the solute (the pentamer fragments of the HET-s and the Aβ fibrils in this study) derived from the 3D-RISM-KH equations, Eqs. 1 and 2, can be represented in the closed analytical form

$$\mu^{\text{solv}} = k_{\text{B}}T\sum_{\gamma}\rho_{\gamma} \times\int d\mathbf{r}\left[\frac{1}{2}h_{\gamma}^{2}(\mathbf{r})\Theta(-h_{\gamma}(\mathbf{r}))- c_{\gamma}(\mathbf{r})-\frac{1}{2}h_{\gamma}(\mathbf{r})c_{\gamma}(\mathbf{r})\right], \quad (3)$$

where $\Theta(x)$ is the Heaviside step function.

Under the isochoric condition, the solvation free energy can be decomposed into the solvation energetic and entropic parts,

$$\mu^{\text{solv}} = \epsilon^{\text{solv}} - TS^{\text{solv}}. \quad (4)$$

The solvation energy ϵ^{solv} can be viewed as, in turn, consisting of two contributions. One contribution arises from creation of a polarized cavity (in pure solvent). The other contribution corresponds to the energy of embedding the solute molecule into the cavity (62). By taking the derivative of μ^{solv} with respect to temperature, we can obtain the entropic component $-TS^{\text{solv}}$ (49,62). We calculated the derivative from the equations obtained by analytical variation of the 3D-RISM-KH and DRISM-KH equations, following Yu et al. (49).

The partial molar volume $\bar{V}$ is obtained from 3D-RISM coupled with the Kirkwood-Buff method (3D-RISM-KB theory) (41), and is expressed in terms of the three-dimensional total correlation functions $c_{\gamma}(\mathbf{r})$ as

$$\bar{V} = k_{\text{B}}T\chi_{\text{T}}\left(1-\rho\sum_{\gamma}\int d\mathbf{r}c_{\gamma}(\mathbf{r})\right), \quad (5)$$

where χ_{T} is the isothermal compressibility of pure solvent, which can be obtained by the RISM theory for the solvent-solvent correlation functions (50).

We considered the protein complexes in ambient water at temperature 298.15 K and pressure 1 bar with the density equal to 0.997 g/cm^3 and the dielectric constant equal to 78. The 3D-RISM-KH equations were solved on a grid of 256^3 points in a cubic supercell of size 128 Å. The cell is large enough to accommodate the fibril fragments along with the sufficient solvation space around them, both in the case of the HET-s prion proteins and of the Aβ peptides. In the 3D-RISM calculations, we used the AMBER ff03 protein force field (57,58) for the HET-s and Aβ proteins, in accord with the energy minimization procedure discussed above. The TIP3P model (63) was used for solvent water molecules. To find the change in the thermodynamic properties of the fibril fragments upon their assembly, we carried out the 3D-RISM calculations for the HET-s and Aβ pentamers as well as for each constituting monomer (referred to as f0 through f4 in each complex). The molecular structures of the fragments and the labeling scheme for the monomers are shown in Fig. 1. The internal energy of proteins was obtained by using the AMBER 9 molecular dynamics package (56), and the total free energy was estimated as the sum of the solvation free energy and the internal energy of the peptides.

RESULTS AND DISCUSSION

Hydration effects on the thermodynamics of the fragments' assembly

The physical mechanisms behind aggregation of fibrillous peptides and the thermodynamic stability of amyloid fibrils have been studied intensively. It is well understood now that the process of formation of amyloid fibril is driven by the hydrophobic effects along with the inter/intrapeptide interactions (including hydrogen bonding, specific and nonspecific electrostatic and dispersion interactions, and possibly, the aromatic bonding). These two factors overcompensate the free energy loss due to the increase in the entropy of proteins upon the association with the subsequent structural changes that accompany the formation of the cross-β morphology of mature fibrils. The same factors are responsible for stability of amyloid fibrils. The molecular dynamics methods can provide extensive information about the thermodynamic properties of biomolecular systems, including aggregates of proteins. At the same time, the quantitative analysis of the solvation effects, in particular, of the solvation entropic contribution to the free energy, remains a notoriously difficult and computationally demanding problem. The 3D-RISM-KH theory provides direct access to the thermodynamic properties, including the solvation entropic effects, based on the analytical representation for the excess chemical potential. It allows us to obtain the quantitative description of the solvation effects for the given experimental conformations without the sampling of the solvent conformational space required in conventional molecular dynamics or Monte Carlo simulations. Below, we present the results of our calculations of the solvation contribution to the free energy for the fragments of the HET-s and Aβ amyloid fibrils, along with their internal energy. The solvation part of the free energy is split up into the energetic and entropic contributions. In the phenomenological approaches, the long-range asymptotics of the first component can be approximately accounted for by the solvent permittivity. In the implicit solvation models, this part of the solvation free energy can be described with a reasonable accuracy, based on the Poisson-Boltzmann

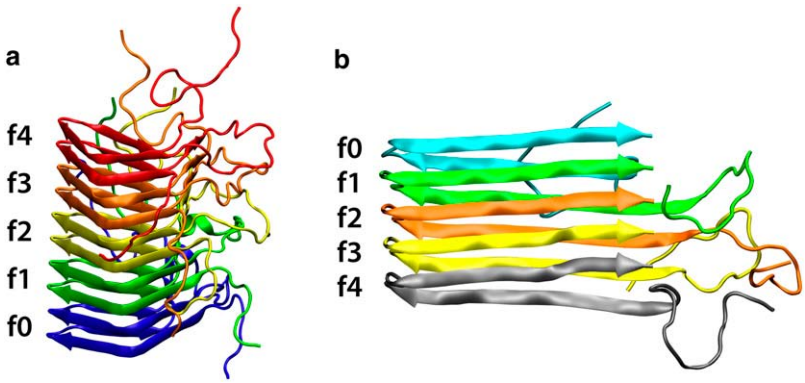

FIGURE 1 Molecular models of (*a*) HET-s pentamer (51) and (*b*) Aβ pentamer (53). This and the following figures were created by using the VMD software (84).

equation, or otherwise, approximated within the Generalized Born model framework.

We summarize the results of our calculations of the solvation free energy for the fragments of the HET-s and Aβ fibrils in Tables 1 and 2, respectively. The results are obtained for the optimized conformations (see the previous section), and thus the internal energies also shown in these tables represent the minimum energy results. The solvation free energy, μ^{solv}, is decomposed into the solvation energy and entropy components, ϵ^{solv} and $-TS^{solv}$, by using Eq. 4. As seen from Table 1, we obtained the negative change in the free energy upon the assembly of the structure from the HET-s monomers (−137 kcal/mol), which means the minimum conformation is stable in water, and the HET-s proteins demonstrate the propensity for aggregation. The association free energy is the result of a delicate balance between the favorable internal energy change (−1483 kcal/mol) and the unfavorable solvation free energy change (+1346 kcal/mol). For the HET-s pentamer studied, the negative change in the solvation entropy is the major component of the free energy change, which stabilizes the solvated structure.

To get further insight into the solvation thermodynamics of the complex, we can compare the different contributions to the solvation free energy and the internal energy. Clearly, the large (compared to the change in the total free energy) negative change in the internal energy is overcompensated by the solvation energy gain, amounting to an unfavorable energy change of 204 kcal/mol. There is a simple explanation to the above cancellation between the solvation contribution to the free energy and the internal energy. First of all, due to the polarization of the solvent, the solvation effects result in the reduction of the direct electrostatic interactions between peptides (phenomenologically described by the solvent dielectric constant). The microscopic solvation effects also need to be accounted for, which is missed in the phenomenological, continuum solvation models. For example, monomers strongly interacting with each other in a complex might have an arrangement of structural water significantly different from the case of disrupted fibril morphology. Another microscopic solvation effect is a change in the network of hydrogen bonds upon solvation of peptides, with the disruption of hydrogen bonds of the bulk solvent, followed by the formation of the network of hydrogen bonds in the proximity of the proteins and between the proteins and water molecules. This effect is one of the major factors contributing to the solvation entropic part of the free energy, and is properly accounted for in the 3D-RISM formalism (64).

TABLE 1 Internal energy, solvation free energy, and total free energy (kcal/mol) of the HET-s pentamer and the constituting monomers in water

		μ^{solv}			
	Internal energy	ϵ^{solv}	$-TS^{solv}$	Total	Free energy
f0	−1096.9	−1740.9	1910.2	169.3	−927.6
f1	−1166.3	−1688.7	1899.9	211.2	−955.1
f2	−1122.5	−1729.2	1900.7	171.5	−951.0
f3	−1163.9	−1666.4	1902.8	236.3	−927.6
f4	−1025.8	−1819.0	1908.7	89.7	−936.1
5-mer	−7058.2	−6956.7	9181.0	2224.3	−4833.9
Association	−1482.8	1687.5	−341.2	1346.3	−136.(5)

The solvation free energy, μ^{solv}, is decomposed into the solvation energy, ϵ^{solv}, and the solvation entropy, $-TS^{solv}$, components. The last row shows the association energies, defined as the difference between the free energy of the pentamer and those of five separate monomers.

TABLE 2 Same as in Table 1, but for the Aβ pentamer

		μ^{solv}			
	Internal energy	ϵ^{solv}	$-TS^{solv}$	Total	Free energy
f0	−73.2	−1059.8	1018.1	−41.7	−114.9
f1	−40.8	−1097.3	1030.0	−67.3	−108.1
f2	−63.5	−1066.3	1027.7	−38.6	−102.1
f3	−132.8	−996.0	1024.5	28.5	−104.4
f4	−102.3	−1053.5	1023.0	−30.5	−132.9
5-mer	−273.9	−5371.5	4821.6	−549.9	−823.8
Association	138.8	−98.6	−301.6	−400.2	−261.(4)

We also analyzed the free energy change upon the assembly for the Aβ peptides in the conformation optimized as discussed above, in the previous section. We found that in this case both the solvation energetic and entropic parts favor the stability of the complex.

Interestingly, the change of the solvation free energy and the internal energy have opposite signs. This is a manifestation of the general thermodynamics Le Chatelier's principle. The solvent responds to the conformational changes of the proteins so as to oppose the factors/forces causing the conformational changes. The unfavorable change in the internal energy can be related to the high charges on individual monomers. Under the physiological conditions, this charge may be compensated by counterions, diminishing the unfavorable electrostatic internal energy contribution. Regardless of that, the contribution of the dispersion, the van der Waals interactions, always favor stability of the complex (∼−890 and −670 kcal/mol for the HET-s and Aβ fragments, respectively). For both the cases investigated here, the solvation entropy change is an essential part of the association free energy, which is in agreement with the experimental (65–69) and the computational studies (14–19,70,71) on amyloid fibrils.

Partial molar volume changes on aggregation

There is experimental evidence that high pressure can disturb the formation of amyloid fibrils and inactivate prion infectivity (66,72–75). In this section, we predict the free energy change under high pressure and elucidate the origin of the pressure effect for the pentamer fragments of the HET-s and Aβ amyloid fibrils.

The pressure effect on proteins can be evaluated as follows. The association free energy $\Delta G^{(P)}$ at arbitrary pressure P can be expressed as (76,77)

$$\Delta G^{(P)} \approx \Delta G^{(P_0)} + (P - P_0)\Delta \bar{V}^{(P_0)}, \quad (6)$$

where $\Delta G^{(P_0)}$ is the association free energy at some reference pressure P_0 (assumed to be the atmospheric pressure in the following), and $\Delta \bar{V}^{(P_0)}$ is the partial molar volume (PMV) change upon the association at the reference pressure. Table 3 presents the partial molar volume $\bar{V}$ and the PMV change for the HET-s and Aβ proteins upon their association predicted by the 3D-RISM-KH theory. We found that the volume change on the association is large and positive for both pentamers (797 and 479 cm^3/mol for HET-s and Aβ, respectively), which is in good agreement with the volumetric measurements on the amyloid fibrils (78–81). Since both the HET-s and Aβ fragments have positive $\Delta \bar{V}^{(P_0)}$, a pressure P less than the reference pressure P_0 will make the second term in the right-hand side of Eq. 6 negative, thus contributing toward negative $\Delta G^{(P)}$ and promoting association of the fragments. Conversely, high pressure P applied to the system will eventually overturn negative $\Delta G^{(P_0)}$ and will result in positive $\Delta G^{(P)}$, followed by destabilization of the fibrils. Our thermodynamic analysis is consistent with the experimentally observed high-pressure effects on the amyloid fibrils (66,73,75).

There are two reasons that can explain the positive volume change:

1. The pentamers have loose intermolecular packing with voids, and disaggregation of the fragments into the monomers eliminates the voids.
2. The pentamers have strong electrostatic intermolecular interactions in the interior domains of the fibrils, and in the process of disaggregation, the polar residues from the fibril core might be exposed to the solvent, resulting in electrostriction of the PMV of the fragment.

To find the cause of the pressure effects, we carried out the 3D-RISM-KH calculations with the electrostatic interactions between peptides and water molecules switched off (only van der Waals interactions between the peptides and water molecules are taken into account). If the former factor is dominant, the volume change should be small. If the latter factor is of major importance, the volume change can be substantial. The results of our calculations are presented in Table 3. $\bar{V}_{LJ}$ is the PMV obtained by applying the 3D-RISM-KH approach to the fragments with all of their partial site charges switched off. $\bar{V}_{Elec}$ is defined as $\bar{V} - \bar{V}_{LJ}$, and thus gives the electrostatic contribution to the partial molar volume change. As it can be seen from the table, even without the electrostriction effects, the PMV changes are large and positive for the both structures (829 and 408 cm^3/mol for the HET-s and Aβ pentamers, respectively). This suggests that factor 1 of the two given above is major in the PMV change, i.e., both the HET-s and Aβ pentamers have loose intermolecular packing with voids. Because the HET-s and Aβ pentamers have the opposite sign of the change $\bar{V}_{Elec}$ on the association, the electrostriction effect on the PMV change may be different for these two complexes. The Aβ pentamer has the positive change in $\bar{V}_{Elec}$ (70 cm^3/mol), suggesting that factor 2, above, also contributes to the positive change in the PMV upon association (the electrostriction effect on the PMV of the pentamer is weaker than that on the PMV of the isolated monomers), while the HET-s pentamer has a negative change (-33 cm^3/mol), which indicates that the electrostriction effect on the PMV of the pentamer is stronger than for the monomers.

TABLE 3 Partial molar volume (PMV) of the HET-s and Aβ pentamers and the constituting monomers in water (cm^3/mol)

	HET-s			Aβ		
	$\bar{V}$	$\bar{V}_{LJ}$	$\bar{V}_{Elec}$	$\bar{V}$	$\bar{V}_{LJ}$	$\bar{V}_{Elec}$
f0	6426.9	6576.4	−149.5	3362.6	3435.5	−72.9
f1	6355.2	6492.4	−137.3	3343.9	3423.8	−79.9
f2	6354.2	6491.7	−137.5	3348.2	3432.8	−84.5
f3	6375.3	6512.0	−136.8	3356.4	3426.4	−70.0
f4	6393.5	6537.0	−143.6	3355.3	3435.9	−80.6
5-mer	32701.6	33438.9	−737.3	17245.2	17562.6	−317.4
Association	796.6	829.3	−32.7	478.7	408.3	70.(5)

The last row shows the PMV change upon the association, defined as the difference between the PMV of pentamer and those of five separate monomers. $\bar{V}$ is the PMV for the full interaction (van der Waals and Coulomb) between the protein and water solvent. $\bar{V}_{LJ}$ is the PMV for the protein with all partial site charges switched off. $\bar{V}_{Elec} = \bar{V} - \bar{V}_{LJ}$ is the electrostatic term in the PMV.

Water channel along the fibril axis

It has been found in the recent molecular dynamics simulations by Buchete et al. (14,15) and Zheng et al. (19) that solvent water molecules can penetrate into the interior cavities along the fibril axis of Aβ fibrils. It was suggested that the interior hydration might play an important role in the structural stability of the Aβ fibrils. Here, we explore this possibility for the Aβ fibrils, and for the first time extend the study of the internal solvation to the HET-s prion fibril. To obtain the three-dimensional molecular picture of solvation, we carried out the analysis of the three-dimensional hydration structure around the Aβ and HET-s pentamers, based on the 3D-RISM-KH approach. It has been shown that this method reproduces the structure of structural water in protein inner spaces in good agreement with x-ray experiment (45).

The results for the Aβ pentamer are presented in Fig. 2. This figure shows the isosurface representation of the three-dimensional hydration structure around the Aβ pentamer predicted by the 3D-RISM-KH theory. The blue surfaces give the areas where the $g(\mathbf{r})$ (the density distribution function) of the water oxygen exceeds the bulk value by a factor of 7. From the peak height of the distribution function, we can estimate—through the 3D-KH closure relation, Eq. 2—the attractive well-depth of binding of the water solvent molecule to the pentamer. For $g(\mathbf{r}) = 7$, for example, it is estimated to be -4 kcal/mol. Thus, the strength of binding of the water molecules at the locations shown in blue in Fig. 2 is >4 kcal/

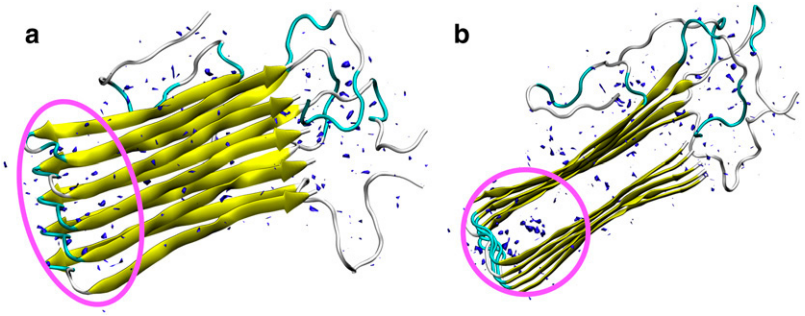

FIGURE 2 Isosurface representation of the three-dimensional hydration structure around the Aβ pentamer, predicted by the 3D-RISM-KH theory: (*a*) side view and (*b*) top view. Blue surfaces show the areas where the density distribution of water oxygen around the Aβ protein exceeds the water bulk density by a factor of 7. Pink circle shows the area corresponding to cavity regions I and III where the hydration was observed in molecular dynamics simulations of Aβ(9-40) fibrils (14).

mol. The pink circle in Fig. 2 indicates the area corresponding to cavity regions I and III, the vicinity of the D23-K28 salt-bridges, where the hydration was observed in the molecular dynamics simulation of the Aβ(9-40) fibrils (15). The hydration structure predicted by the 3D-RISM-KH theory is in excellent agreement with the molecular dynamics simulations (14,15,19).

Analyzing the three-dimensional hydration structure around the HET-s pentamer, we found that the highest peak of the distribution function $g(\mathbf{r})$ for water oxygen is located at the position localized near E234, G269, and S273 residues of f3 fragment of the pentamer (the labeling scheme has been explained in Methods). From the peak height ($g(\mathbf{r}) \approx 29$), the depth of the attractive well is estimated to be -17 kcal/mol. The most probable orientation of the water molecule in this peak shown in Fig. 3 was reconstructed, based on the distribution-function peak positions of both the water oxygen and hydrogen sites. We also located and assigned the water molecules in similar positions for each monomers (see Fig. 4). These water molecules are bound to the pentamer with a binding strength of 6 kcal/mol and more, which is indicative of a possibility of formation of a water channel along the fibril axis of the HET-s fibrillous fragment, similar to what has been observed for the Aβ fibril.

Interestingly, both the HET-s and Aβ fibrils can accommodate the solvent molecules in the channel in the interior region. These solvent (water) molecules are strongly bound and integrated into the structure, as shown in Fig. 3. Therefore, losing these structural water molecules could cause structural changes in the aggregates. Our theoretical observation strongly supports that the interior hydration may play an important role in the structural stability of the HET-s and Aβ fibrils.

CONCLUDING REMARKS

Using the statistical mechanical, three-dimensional molecular theory of solvation, we analyzed the thermodynamic stability and hydration properties of the experimental structures of the fragments of the HET-s prion amyloid fibril (51) and Aβ fibril (53). The HET-s prion protein is the infectious element of the filamentous fungus *Podospora anserina*. The Aβ protein is the major component of Alzheimer's disease-associated plaques. To provide an insight into the physical mechanisms behind the stability of these experimental structures, we decompose the association free energy, defined as the difference between the free energy of a complex and the free energy of the constituting monomers, into the energetic and the hydration entropic contributions. The latter is directly related to the hydrophobic effects, which play an essential role in the aggregation of proteins (13,82,83). We show that the change in the total free energy upon association is a result of the delicate balance between the internal energy and the hydration free energy. We give the quantitative description of the hydrophobic cooperativity (long time known as the driving force of the oligomerization). By calculating the partial molar volume, we found that the volume change upon the association for the both pentamers is large and positive, which suggests that high pressure destabilizes the aggregates. This observation is in good agreement with the

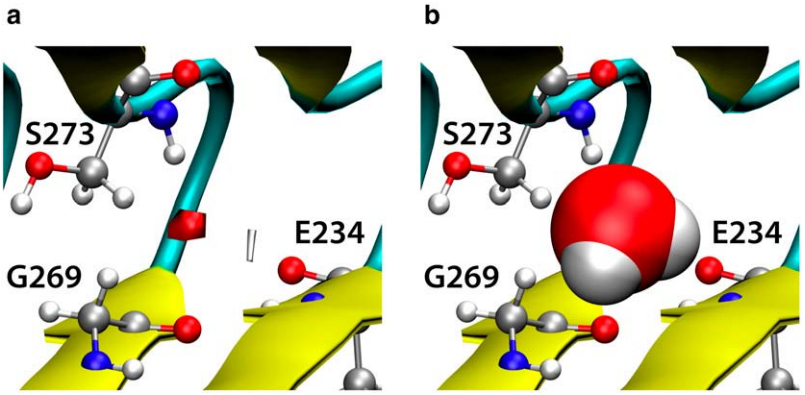

FIGURE 3 (*a*) Isosurface representation of the three-dimensional hydration structure predicted by the 3D-RISM-KH theory. (*b*) The most probable arrangement of the water molecule in proximity of residues E234, G269, and S273 of monomer f3 in the HET-s pentamer. In panel *a*, red and white surfaces show the areas where the density distribution of, respectively, water oxygen and hydrogen around the HET-s protein, exceeds the water bulk density by a factor of 3.

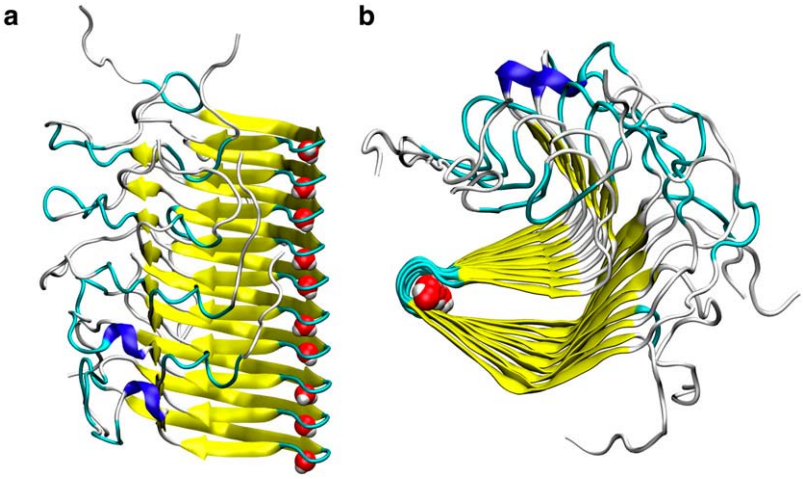

FIGURE 4 Water channel along the fibril axis of the HET-s pentamer, predicted by the 3D-RISM-KH theory. (*a*) side view, and (*b*) top view.

available experimental results. From the analysis of the hydration structure around the aggregates, we found that both the HET-s and Aβ pentamers have loose intermolecular packing with voids. The three-dimensional molecular theory of solvation reveals the three-dimensional hydration structure around the proteins and predicts that the water molecules may be locked in the interior cavities along the fibril axis for both HET-s and Aβ proteins. For the Aβ peptides, our results are in agreement with the previous all-atom molecular dynamics simulations (14,15,19). For the HET-s prions, we identify the water channels for the first time. The interior water molecules are strongly bound and integrated into the fibril structure. We suggest that the interior hydration plays an important role in the structural stability of fibrils.

We are grateful to Drs. Beat H. Meier and Hélène Van Melckebeke for providing the PDB coordinates of the experimental structure of the HET-s protein.

We acknowledge the financial support by the Alberta Prion Research Institute and the National Research Council of Canada. The computations were supported by the Center of Excellence in Integrated Nanotools at the University of Alberta.

REFERENCES

1. Dobson, C. M. 2001. The structural basis of protein folding and its links with human disease. *Philos. Trans. R. Soc. Lond. B Biol. Sci.* 356:133–145.
2. Caughey, B., and P. T. Lansbury. 2003. Protofibrils, pores, fibrils, and neurodegeneration: separating the responsible protein aggregates from the innocent bystanders. *Annu. Rev. Neurosci.* 26:267–298.
3. Jahn, T. R., and S. E. Radford. 2008. Folding versus aggregation: polypeptide conformations on competing pathways. *Arch. Biochem. Biophys.* 469:100–117.
4. Aguzzi, A., and M. Heikenwalder. 2006. Pathogenesis of prion diseases: current status and future outlook. *Nat. Rev. Microbiol.* 4:765–775.
5. Millhauser, G. L. 2007. Copper and the prion protein: methods, structures, function, and disease. *Annu. Rev. Phys. Chem.* 58:299–320.
6. Silveira, J. R., G. J. Raymond, A. G. Hughson, R. E. Race, V. L. Sim, S. F. Hayes, and B. Caughey. 2005. The most infectious prion protein particles. *Nature.* 437:257–261.
7. Zerovnik, E. 2002. Amyloid fibril formation. proposed mechanisms and relevance to conformational disease. *Eur. J. Biochem.* 269:3362–3371.
8. Sipe, J. D., and A. S. Cohen. 2000. Review: history of the amyloid fibril. *J. Struct. Biol.* 130:88–98.
9. Auer, S., C. M. Dobson, and M. Vendruscolo. 2007. Characterization of the nucleation barriers for protein aggregation and amyloid formation. *HFSP J.* 1:137–146.
10. Jarrett, J. T., and P. T. Lansbury. 1993. Seeding ''one-dimensional crystallization'' of amyloid: a pathogenic mechanism in Alzheimer's disease and scrapie? *Cell.* 73:1055–1058.
11. Meinhardt, J., G. G. Tartaglia, A. Pawar, T. Christopeit, P. Hortschansky, V. Schroeckh, C. M. Dobson, M. Vendruscolo, and M. Fandrich. 2007. Similarities in the thermodynamics and kinetics of aggregation of disease-related Aβ(1–40) peptides. *Protein Sci.* 16:1214–1222.
12. Sunde, M., L. C. Serpell, M. Bartlam, P. E. Fraser, M. B. Pepys, and C. C. F. Blake. 1997. Common core structure of amyloid fibrils by synchrotron x-ray diffraction. *J. Mol. Biol.* 273:729–739.
13. Hills, R. D., Jr., and C. L. Brooks III. 2007. Hydrophobic cooperativity as a mechanism for amyloid nucleation. *J. Mol. Biol.* 368:894–901.
14. Buchete, N.-V., R. Tycko, and G. Hummer. 2005. Molecular dynamics simulations of Alzheimer's β-amyloid protofilaments. *J. Mol. Biol.* 353:804–821.
15. Buchete, N.-V., and G. Hummer. 2007. Structure and dynamics of parallel β-sheets, hydrophobic core, and loops in Alzheimer's Aβ fibrils. *Biophys. J.* 92:3032–3039.
16. Hwang, W., S. Zhang, R. D. Kamm, and M. Karplus. 2004. Kinetic control of dimer structure formation in amyloid fibrillogenesis. *Proc. Natl. Acad. Sci. USA.* 101:12916–12921.
17. Klimov, D. K., and D. Thirumalai. 2003. Dissecting the assembly of Aβ_{16-22} amyloid peptides into antiparallel β sheets. *Structure.* 11: 295–307.
18. Ma, B., and R. Nussinov. 2006. The stability of monomeric intermediates controls amyloid formation: Aβ25–35 and its N27Q mutant. *Biophys. J.* 90:3365–3374.
19. Zheng, J., H. Jang, B. Ma, C.-J. Tsai, and R. Nussinov. 2007. Modeling the Alzheimer Aβ_{17-42} fibril architecture: tight intermolecular sheet-sheet association and intramolecular hydrated cavities. *Biophys. J.* 93:3046–3057.
20. Nguyen, P. H., M. S. Li, G. Stock, J. E. Straub, and D. Thirumalai. 2007. Monomer adds to preformed structured oligomers of Aβ-peptides by a two-stage dock-lock mechanism. *Proc. Natl. Acad. Sci. USA.* 104:111–116.
21. Dima, R. I., and D. Thirumalai. 2004. Probing the instabilities in the dynamics of helical fragments from mouse PrPC. *Proc. Natl. Acad. Sci. USA.* 101:15335–15340.

22. DeMarco, M., and V. Daggett. 2007. Molecular mechanism for low pH triggered misfolding of the human prion protein. *Biochemistry.* 46: 3045–3054.

23. DeMarco, M. L., and V. Daggett. 2004. From conversion to aggregation: protofibril formation of the prion protein. *Proc. Natl. Acad. Sci. USA.* 101:2293–2298.

24. Langella, E., R. Improta, and V. Barone. 2004. Checking the pH-induced conformational transition of prion protein by molecular dynamics simulations: effect of protonation of histidine residues. *Biophys. J.* 87:3623–3632.

25. De Simone, A., A. Zagari, and P. Derreumaux. 2007. Structural and hydration properties of the partially unfolded states of the prion protein. *Biophys. J.* 93:1284–1292.

26. Flöck, D., S. Colacino, G. Colombo, and A. D. Nola. 2006. Misfolding of the amyloid β-protein: a molecular dynamics study. *Proteins.* 62:183–192.

27. Tsai, H.-H. G., M. Reches, C.-J. Tsai, K. Gunasekaran, E. Gazit, and R. Nussinov. 2005. Energy landscape of amyloidogenic peptide oligomerization by parallel-tempering molecular dynamics simulation: significant role of ASN ladder. *Proc. Natl. Acad. Sci. USA.* 102: 8174–8179.

28. Ma, B., and R. Nussinov. 2002. Stabilities and conformations of Alzheimer's β-amyloid peptide oligomers (Aβ 16–22, Aβ 16–35, and Aβ 10–35): sequence effects. *Proc. Natl. Acad. Sci. USA.* 99:14126–14131.

29. Itoh, S., and Y. Okamoto. 2008. Amyloid-β(29–42) dimer formations studied by a multicanonical-multioverlap molecular dynamics simulation. *J. Phys. Chem. B.* 112:2767–2770.

30. Daidone, I., F. Simona, D. Roccatano, R. A. Broglia, G. Tiana, G. Colombo, and A. D. Nola. 2004. β-Hairpin conformation of fibrillogenic peptides: structure and α-β transition mechanism revealed by molecular dynamics simulations. *Proteins.* 57:198–204.

31. Wei, G., N. Mousseau, and P. Derreumaux. 2007. Computational simulations of the early steps of protein aggregation. *Prion.* 1:3–8.

32. Hall, C. K., and V. A. Wagoner. 2006. Computational approaches to fibril structure and formation. *Methods Enzymol.* 412:338–365.

33. Röhrig, U. F., A. Laio, N. Tantalo, M. Parrinello, and R. Petronzio. 2006. Stability and structure of oligomers of the Alzheimer peptide Aβ16–22: from the dimer to the 32-mer. *Biophys. J.* 91:3217–3229.

34. Ma, B., and R. Nussinov. 2002. Molecular dynamics simulations of alanine rich β-sheet oligomers: insight into amyloid formation. *Protein Sci.* 11:2335–2350.

35. Kovalenko, A. 2003. Three-dimensional RISM theory for molecular liquids and solid-liquid interfaces. *In* Molecular Theory of Solvation. Vol. 24 of Understanding Chemical Reactivity. F. Hirata, editor. Kluwer Academic Publishers, Dordrecht, The Netherlands.

36. Beglov, D., and B. Roux. 1995. Numerical solution of the hypernetted chain equation for a solute of arbitrary geometry in three dimensions. *J. Chem. Phys.* 103:360–364.

37. Kovalenko, A., and F. Hirata. 1998. Three-dimensional density profiles of water in contact with a solute of arbitrary shape: a RISM approach. *Chem. Phys. Lett.* 290:237–244.

38. Kovalenko, A., and F. Hirata. 1999. Self-consistent description of a metal-water interface by the Kohn-Sham density functional theory and the three-dimensional reference interaction site model. *J. Chem. Phys.* 110:10095–10112.

39. Kovalenko, A., and F. Hirata. 2000. Potentials of mean force of simple ions in ambient aqueous solution. I. three-dimensional reference interaction site model approach. *J. Chem. Phys.* 112:10391–10402.

40. Drabik, P., S. Gusarov, and A. Kovalenko. 2007. Microtubule stability studied by three-dimensional molecular theory of solvation. *Biophys. J.* 92:394–403.

41. Harano, Y., T. Imai, A. Kovalenko, M. Kinoshita, and F. Hirata. 2001. Theoretical study for partial molar volume of amino acids and polypeptides by the three-dimensional reference interaction site model. *J. Chem. Phys.* 114:9506–9511.

42. Imai, T., Y. Harano, M. Kinoshita, A. Kovalenko, and F. Hirata. 2007. Theoretical analysis on changes in thermodynamic quantities upon protein folding: essential role of hydration. *J. Chem. Phys.* 126:225102.

43. Imai, T., Y. Harano, A. Kovalenko, and F. Hirata. 2001. Theoretical study for volume changes associated with the helix-coil transition of polypeptides. *Biopolymers.* 59:512–519.

44. Imai, T., H. Isogai, T. Seto, A. Kovalenko, and F. Hirata. 2006. Theoretical study of volume changes accompanying xenon-lysozyme binding: implication for molecular mechanism of pressure reversal of anesthesia. *J. Phys. Chem. B.* 110:12149–12154.

45. Imai, T., R. Hiraoka, A. Kovalenko, and F. Hirata. 2005. Water molecules in a protein cavity detected by a statistical-mechanical theory. *J. Am. Chem. Soc.* 127:15334–15335.

46. Yamazaki, T., T. Imai, F. Hirata, and A. Kovalenko. 2007. Theoretical study of cosolvent effect on the partial molar volume change of staphylococcal nuclease associated with pressure denaturation. *J. Phys. Chem. B.* 111:1206–1212.

47. Chandler, D., and H. C. Andersen. 1972. Optimized cluster expansions for classical fluids. II. Theory of molecular liquids. *J. Chem. Phys.* 57:1930–1937.

48. Chandler, D. 1973. Derivation of an integral equation for pair correlation functions in molecular fluids. *J. Chem. Phys.* 59:2742–2746.

49. Yu, H.-A., B. Roux, and M. Karplus. 1990. Solvation thermodynamics: an approach from analytical temperature derivatives. *J. Chem. Phys.* 92:5020–5033.

50. Hansen, J. P., and I. R. McDonald. 1986. Theory of Simple Liquids. Academic Press, London, United Kingdom.

51. Wasmer, C., A. Lange, H. V. Melckebeke, A. B. Siemer, R. Riek, and B. H. Meier. 2008. Amyloid fibrils of the HET-s(218–289) prion form a β solenoid with a triangular hydrophobic core. *Science.* 319:1523–1526.

52. Petkova, A. T., Y. Ishii, J. J. Balbach, O. N. Antzutkin, R. D. Leapman, F. Delaglio, and R. Tycko. 2002. A structural model for Alzheimer's β-amyloid fibrils based on experimental constraints from solid state NMR. *Proc. Natl. Acad. Sci. USA.* 99:16742–16747.

53. Lührs, T., C. Ritter, M. Adrian, D. Riek-Loher, B. Bohrmann, H. Döbeli, D. Schubert, and R. Riek. 2005. 3D structure of Alzheimer's amyloid-β(1–42) fibrils. *Proc. Natl. Acad. Sci. USA.* 102:17342–17347.

54. Fiser, A., R. K. Do, and A. Sali. 2000. Modeling of loops in protein structures. *Protein Sci.* 9:1753–1773.

55. Fiser, A., and A. Sali. 2003. ModLoop: automated modeling of loops in protein structures. *Bioinformatics.* 19:2500–2501.

56. Case, D. A., T. E. Cheatham III, T. Darden, H. Gohlke, R. Luo, K. M. Merz, Jr., A. Onufriev, C. Simmerling, B. Wang, and R. J. Woods. 2005. The AMBER biomolecular simulation programs. *J. Comput. Chem.* 26:1668–1688.

57. Duan, Y., C. Wu, S. Chowdhury, M. C. Lee, G. Xiong, W. Zhang, R. Yang, P. Cieplak, R. Luo, T. Lee, J. Caldwell, J. Wang, and P. A. Kollman. 2003. A point-charge force field for molecular mechanics simulations of proteins based on condensed-phase quantum mechanical calculations. *J. Comput. Chem.* 24:1999–2012.

58. Lee, M. C., and Y. Duan. 2004. Distinguish protein decoys by using a scoring function based on a new AMBER force field, short molecular dynamics simulations, and the generalized Born solvent model. *Proteins.* 55:620–634.

59. Onufriev, A., D. Bashford, and D. A. Case. 2004. Exploring protein native states and large-scale conformational changes with a modified generalized born model. *Proteins.* 55:383–394.

60. Feig, M., A. Onufriev, M. S. Lee, W. Im, D. A. Case, and C. L. Brooks III. 2004. Performance comparison of generalized born and Poisson methods in the calculation of electrostatic solvation energies for protein structures. *J. Comput. Chem.* 25:265–284.

61. Perkyns, J. S., and B. M. Pettitt. 1992. A site-site theory for finite concentration saline solutions. *J. Chem. Phys.* 97:7656–7666.

62. Pettitt, B. M., and P. J. Rossky. 1986. Alkali halides in water: ion-solvent correlations and ion-ion potentials of mean force at infinite dilution. *J. Chem. Phys.* 84:5836–5844.

63. Jorgensen, W. L., J. Chandrasekhar, J. D. Madura, R. W. Impey, and M. L. Klein. 1983. Comparison of simple potential functions for simulating liquid water. *J. Chem. Phys.* 79:926–935.

64. Hirata, F. 2003. Theory of molecular liquids. *In* Molecular Theory of Solvation, Understanding Chemical Reactivity, Vol. 24. F. Hirata, editor. Kluwer Academic Publishers, Dordrecht, The Netherlands.

65. Kardos, J., K. Yamamoto, K. Hasegawa, H. Naiki, and Y. Goto. 2004. Direct measurement of the thermodynamic parameters of amyloid formation by isothermal titration calorimetry. *J. Biol. Chem.* 279: 55308–55314.

66. Dirix, C., F. Meersman, C. E. MacPhee, C. M. Dobson, and K. Heremans. 2005. High hydrostatic pressure dissociates early aggregates of $TTR_{105–115}$, but not the mature amyloid fibrils. *J. Mol. Biol.* 347:903–909.

67. Sasahara, K., H. Naiki, and Y. Goto. 2005. Kinetically controlled thermal response of β_2-microglobulin amyloid fibrils. *J. Mol. Biol.* 352:700–711.

68. Meersman, F., and C. M. Dobson. 2006. Probing the pressure-temperature stability of amyloid fibrils provides new insights into their molecular properties. *Biochim. Biophys. Acta.* 1764:452–460.

69. Lin, M.-S., L.-Y. Chen, H.-T. Tsai, S. S.-S. Wang, Y. Chang, A. Higuchi, and W.-Y. Chen. 2008. Investigation of the mechanism of β-amyloid fibril formation by kinetic and thermodynamic analyses. *Langmuir.* 24:5802–5808.

70. Kinoshita, M. 2004. Ordered aggregation of big bodies with high asphericity in small spheres: a possible mechanism of the amyloid fibril formation. *Chem. Phys. Lett.* 387:54–60.

71. Tarus, B., J. E. Straub, and D. Thirumalai. 2005. Probing the initial stage of aggregation of the $A\beta_{10–35}$-protein: assessing the propensity for peptide dimerization. *J. Mol. Biol.* 345:1141–1156.

72. Brown, P., R. Meyer, F. Cardone, and M. Pocchiari. 2003. Ultra-high-pressure inactivation of prion infectivity in processed meat: a practical method to prevent human infection. *Proc. Natl. Acad. Sci. USA.* 100:6093–6097.

73. Fernández García, A., P. Heindl, H. Voigt, M. Büttner, D. Wienhold, P. Butz, J. Stärke, B. Tauscher, and E. Pfaff. 2004. Reduced proteinase K resistance and infectivity of prions after pressure treatment at 60°C. *J. Gen. Virol.* 85:261–264.

74. Fernandez Garcia, A., P. Heindl, H. Voigt, M. Büttner, P. Butz, N. Tauber, B. Tauscher, and E. Pfaff. 2005. Dual nature of the infectious prion protein revealed by high pressure. *J. Biol. Chem.* 280:9842–9847.

75. Torrent, J., C. Balny, and R. Lange. 2006. High pressure modulates amyloid formation. *Protein Pept. Lett.* 13:271–277.

76. Balny, C., P. Masson, and K. Heremans. 2002. High pressure effects on biological macromolecules: from structural changes to alteration of cellular processes. *Biochim. Biophys. Acta.* 1595:3–10.

77. Royer, C. A. 2002. Revisiting volume changes in pressure-induced protein unfolding. *Biochim. Biophys. Acta.* 1595:201–209.

78. Niraula, T. N., T. Konno, H. Yamada, K. Akasaka, and H. Tachibana. 2004. Pressure-dissociable reversible assembly of intrinsically denatured lysozyme is a precursor for amyloid fibrils. *Proc. Natl. Acad. Sci. USA.* 101:4089–4093.

79. Kamatari, Y. O., S. Yokoyama, H. Tachibana, and K. Akasaka. 2005. Pressure-jump NMR study of dissociation and association of amyloid protofibrils. *J. Mol. Biol.* 349:916–921.

80. Abdul Latif, A. R., R. Kono, H. Tachibana, and K. Akasaka. 2007. Kinetic analysis of amyloid protofibril dissociation and volumetric properties of the transition state. *Biophys. J.* 92:323–329.

81. Akasaka, K., A. R. Abdul Latif, A. Nakamura, K. Matsuo, H. Tachibana, and K. Gekko. 2007. Amyloid protofibril is highly voluminous and compressible. *Biochemistry.* 46:10444–10450.

82. Chothia, C. 1974. Hydrophobic bonding and accessible surface area in proteins. *Nature.* 248:338–339.

83. Chandler, D. 2005. Interfaces and the driving force of hydrophobic assembly. *Nature.* 437:640–647.

84. Humphrey, W., A. Dalke, and K. Schulten. 1996. VMD: visual molecular dynamics. *J. Mol. Graph.* 14:33–38.